INPE – National Institute for Space Research
São José dos Campos – SP – Brazil – May 16-20, 2016

NONLINEAR FREE VIBRATIONS OF SHEAR DEFORMABLE BEAMS WITH AXIALLY MOVABLE BOUNDARY CONDITIONS

Stefano Lenci[1], Francesco Clementi[2], Giuseppe Rega[3]

[1]Department of Civil and Building Engineering, and Architecture, Polytechnic University of Marche, Ancona, Italy, lenci@univpm.it
[2]Department of Civil and Building Engineering, and Architecture, Polytechnic University of Marche, Ancona, Italy, francesco.clementi@univpm.it
[3]Department of Structural and Geotechnical Engineering, Sapienza University of Rome, Rome, Italy, giuseppe.rega@uniroma1.it

Abstract: The nonlinear free oscillations of a planar Timoshenko beam with axially movable boundary conditions are studied, by adding an axial spring at one hand in order to simulate the effect of an elastic constraint with stiffness κ. Since the exact solution is not available, two different approximate solutions are compared (analytical and numerical). The comparison is made in terms of backbone curves for both solutions. Attention is focused on the effect of the beam slenderness, by considering both slender and stubby beams, and on the effect of the ending spring stiffness κ, with values $0 \leq \kappa \leq \infty$. A very good agreement between the two solutions is highlighted, together with their reliability.

Keywords: Analysis and Control of Nonlinear Dynamical Systems with Practical Applications, Nonlinear Dynamics and Complex Systems, Nonlinear Dynamics of Systems with Infinite Dimension, Nonlinear Oscillations, Backbone Curve.

1. BASIC INFORMATION

This work investigates the nonlinear free oscillations of a planar beam, starting from the observation that beams with one axially free end display a softening nonlinear behavior, while beams axially restrained exhibit a hardening nonlinear behavior. This difference, already reported by Atluri [1], is a peculiarity of the nonlinear regime. Luongo et al. [2] addressed the same problem by the Galerkin method, while Lacarbonara and Yabuno [3] applied the multiple scale method directly to the governing PDEs and provided an experimental verification of the phenomenon. Previous works considered slender beams, and perfectly restrained vs perfectly unrestrained boundary conditions. These limitations have been removed by the authors [4].

In order to revisit the whole matter beyond the topic of slender structures, a Timoshenko beam model is considered, by taking into account axial and rotational inertia, as well as axial and shear stiffnesses. Moreover, an axial spring is added at one end to simulate the effect of an elastic constraint with stiffness κ. The limit cases of axially free and axially constrained boundary conditions are obtained for κ=0 and $\kappa \rightarrow \infty$, respectively.

Since the exact solution is not available, two different approximate solutions are compared. The first is obtained with the asymptotic development method, in particular the Poincaré-Lindstedt method, and is analytical. The second is obtained by the Finite Element Method, and is purely numerical, with the aid of a commercial software.

The comparison is made in terms of backbone curves, namely the curves that describe the amplitude dependence of the nonlinear frequency, which are obtained both analytically and numerically. Attention is focused on the effect of the slenderness of the beam, by considering both slender and stubby beams, and of the varying stiffness κ of the end spring.

A very good agreement between the two different approximate solutions is highlighted, and we can conclude that both are reliable. In particular, the comparison shows the effectiveness of the analytical solution, which can thus be used for systematic parametric investigations. In this respect, regions of hardening or softening behavior in parameters space are identified.

2. EQUATIONS OF MOTION

The following kinematically exact governing equations have been obtained in [4] for the free oscillations of a planar, linearly elastic, initially straight Timoshenko beam:

$$\left\{EA\left[\sqrt{(1+W')^2+U'^2}-1\right]\frac{1+W'}{\sqrt{(1+W')^2+U'^2}}+GA\left[\theta-\arctan\left(\frac{U'}{1+W'}\right)\right]\frac{1+W'}{\sqrt{(1+W')^2+U'^2}}\right\}'=\rho A\ddot{W},$$

$$\left\{EA\left[\sqrt{(1+W')^2+U'^2}-1\right]\frac{U'}{\sqrt{(1+W')^2+U'^2}}-GA\left[\theta-\arctan\left(\frac{U'}{1+W'}\right)\right]\frac{1+W'}{\sqrt{(1+W')^2+U'^2}}\right\}'=\rho A\ddot{U}, \quad (1)$$

$$\left[EJ\frac{\theta'}{\sqrt{(1+W')^2+U'^2}}\right]'-GA\left[\theta-\arctan\left(\frac{U'}{1+W'}\right)\right]\sqrt{(1+W')^2+U'^2}=\rho J\ddot{\theta},$$

where $W(Z,T)$, $U(Z,T)$ and $\theta(Z,T)$ are the axial and the transversal displacements of the beam axis and the rotation of the cross-section, respectively. Z is the spatial coordinate in the rest rectilinear configuration, which ranges from 0 to the length L, T is the time, prime means derivative with respect to Z and dot means derivative with respect to T. EA, GA and EJ are the axial, shear and bending stiffnesses, respectively.

The considered boundary conditions are (H_0 is the horizontal internal force and M is the bending moment).

$$W(0,T)=0, \qquad H_0(L,T)+\kappa W(L,T)=0,$$
$$U(0,T)=0, \qquad U(L,T)=0,$$
$$M(0,T)=0, \qquad M(L,T)=0. \quad (2)$$

The beam (see Fig. 1) is axially fixed at the left end (Z=0), while it has an axial linear spring, of stiffness κ, at the right end (Z=L).

Figure 1 – Current configuration of the initially straight beam with end spring

The previous equations and boundary conditions have been solved approximately by the Poincaré-Lindstedt method, up to the third order, to obtain the linear frequency ω_0 and the nonlinear correction coefficient ω_2. The details of the computations are reported in [5], where the following dimensionless parameters (l slenderness of the beam, z measure of the shear stiffness and κ_h stiffness of the axial spring) are used:

$$l=L\sqrt{A/J}\,, z=1/[2(1+\nu)\chi],$$
$$\kappa_h=\kappa\, L^3/EJ. \quad (3)$$

3. ANALYTICAL APPROXIMATE SOLUTION

The approximate analytical solution is determined in [4,5] by means of the Poincaré-Lindstedt asymptotic development method [6]. To apply the method, it is first necessary to introduce the rescaled dimensionless time $t = \omega T$. Then, the solution is sought after in the form

$$U(Z,t)=\varepsilon U_1(Z,t)+\varepsilon^2 U_2(Z,t)+\varepsilon^3 U_3(Z,t)+\ldots,$$
$$W(Z,t)=\varepsilon W_1(Z,t)+\varepsilon^2 W_2(Z,t)+\varepsilon^3 W_3(Z,t)+\ldots,$$
$$\theta(Z,t)=\varepsilon\theta_1(Z,t)+\varepsilon^2\theta_2(Z,t)+\varepsilon^3\theta_3(Z,t)+\ldots,$$
$$\omega=\omega_0+\varepsilon\omega_1+\varepsilon^2\omega_2+\ldots, \quad (4)$$

where ε is a small parameter underlining the fact that we are looking for moderate (and not large) amplitude oscillations. It is worth to remark that it is just the first non-vanishing nonlinear correction coefficient ω_2 that governs the nonlinear behaviour, which is softening for $\omega_2 < 0$ and hardening for $\omega_2 > 0$.

We have assumed the transversal behavior as dominant with respect to the axial one (i.e., W_1=0), and have considered terms only up to the third order.

The result of lengthy computations is

$$\omega=\sqrt{\frac{E}{\rho}\frac{1}{L^2}}\sqrt{\frac{J}{A}}\left[\bar{\omega}_0+\left(\frac{\varepsilon U_a}{L}\right)^2+\bar{\omega}_2+\cdots\right]. \quad (5)$$

where U_a is the amplitude of the first order solution.

Since in the numerical simulations we will assume ν = 0.3 and a rectangular cross-section (χ = 1.2), we have z = 0.3205 (note that for a rectangular cross-section z ranges from z = 0.417 for ν = 0 to z = 0.28 for ν = 0.5, namely, it is weakly dependent on the Poisson coefficient). Thus, in the problem we have only the two parameters l, the slenderness, and κ_h, the spring stiffness.

4. NUMERICAL APPROXIMATE SOLUTION

In this section, a FEM solution is obtained with the commercial software MIDAS Gen©. A standard Timoshenko beam element in large displacements 2D framework is considered, with an isotropic linearly elastic material. These hypotheses are consistent with the model reported in Sect. 2. Each finite element has 3 degrees of freedom (d.o.f.), 1 translation along the axis, 1 translation perpendicular to the axis and 1 rotation.

While the analytical computations refer to any beam, for the numerical simulations we need to choose a material and a cross-section. The beam is made of steel, and it has rectangular cross-section of width B = 20 cm and varying thickness H and length L. Thus, we have:

- ρ = 7850 kg/m^3, the density of material of the beam;
- $E = 2.1 \times 10^{11}$ N/m^2, the Young modulus;
- ν = 0.3, the Poisson coefficient;
- χ = 1.2, the shear correction factor.

These values give

$$\omega=\sqrt{\frac{E}{\rho}}=5172\ m/sec,\ z{=}0.3205. \quad (6)$$

Since the objective of the simulations is to correlate the response amplitude with the (free) nonlinear vibration frequency, in order to build numerically the backbone curve (to be compared with its analytical counterpart (5)), we have considered free nonlinear vibrations with zero initial velocity and a prescribed initial displacement equal to the first modal shape. Thus, the initial displacement is given by

$$U(Z,0) = U_a sin\left(\frac{\pi Z}{L}\right) \tag{7}$$

which is the first linear mode. It is worth to remark that this introduces an approximation, since it is known that the nonlinear normal mode differs from the linear one [7]. However, our results will show that for the moderately large displacements considered in this work this difference is negligible.

To detect the vibration frequency associated with a given amplitude U_a, one should determine the period from the time history, thus getting one point of the backbone curve. Then, the simulation should be repeated with a different initial amplitude. This procedure is very time consuming, and thus we decided to proceed in a different way.

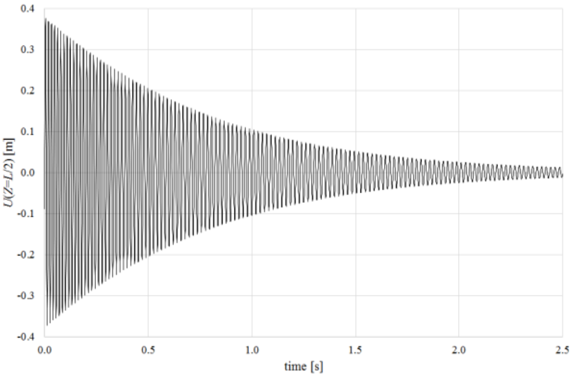

a)

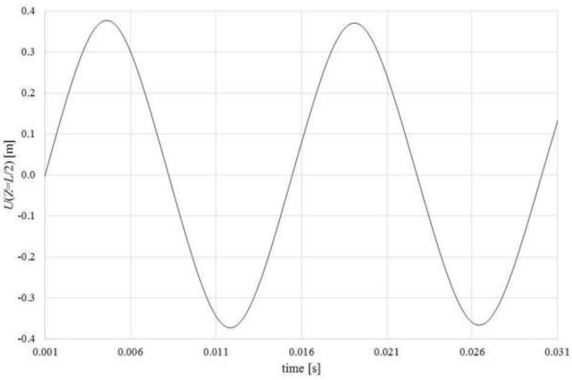

b)

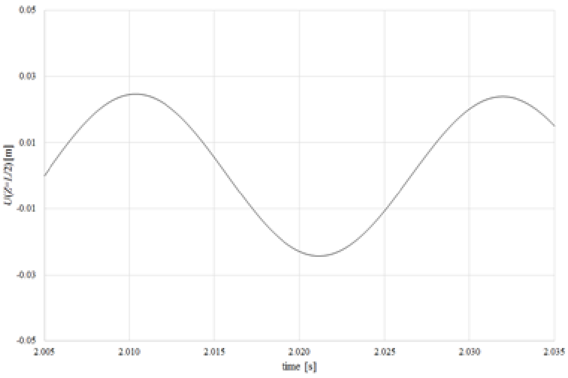

c)

Figure 2 – Numerical time histories for L = 5 m and H = 50 cm (l = 34.610). Spatial step ΔZ = 5 cm, time step ΔT = 0.0005 sec, hinged-hinged boundary conditions.

We introduced a very small damping. From one side, this stabilizes the numerical solution, and from the other side this reduces (slowly) the amplitude of the oscillations, thus covering within a single time history the whole range of amplitudes from the applied U_a to 0.

We considered a damping coefficient equal to ξ = 0.005, which is very small and guarantees that the decrement of the amplitude can be neglected within each half oscillation.

The numerically obtained time history $U(Z{=}L/2, t)$ of the point of maximum amplitude is then post-processed, searching for the zeros of this function. The difference between two consecutive zeros represents the local semi-period, or the local double of the frequency. The maximum of the function in a time interval is the associated amplitude. We thus obtained a candidate point of the backbone curve. Before accepting it, we checked that there were no other maxima within the considered time interval, that would reflect the presence of subharmonic spurious (and unwanted) oscillations excited by the nonlinear coupling between the first (directly excited) and higher order (not directly excited) modes.

The adopted procedure is easy and fast (we do it automatically), and permits us to get a full backbone curve from a single time history, i.e. from a single run of the software. The procedure is illustrated in Fig. 2. In Fig. 2a it is reported the full time history, that lasts 2.5 sec. The decrement of the amplitude due to damping is clearly visible in this full scale figure.

In Fig. 2b an initial 0.03 sec window of the time history is reported, while in Fig. 2c a 0.03 sec window starting from T = 2.005 sec is depicted. In both figures it is possible to see that two consecutive peaks have approximately the same amplitude, i.e. at the scale of the period the damping does not influence significantly the amplitude. On the contrary, for different amplitudes the period (and thus the frequency) strongly varies, as shown by the comparison between Figs. 2b and 2c.

In Fig. 2b the first two time instants in which the displacement is zero are T_1 = 0.000592 sec and T_2 = 0.007813 sec, so that the local circular frequency is $\omega = \pi/(T_2 - T_1)$= 435.08 rad/sec. In this half period the maximum displacement is U_a = 0.375 m. We have thus obtained the first point of the backbone curve. The same reasoning applied to Fig. 2c gives T_1 = 2.005022 sec, T_2 = 2.015806 sec → $\omega = \pi/(T_2 - T_1)$ = 291.3 rad/sec, and U_a = 0.02465 m.

Repeating the same procedure for all the half-waves of the time history, we finally get the numerical backbone curve.

The maximum displacement is $U_{a,max}$ = 0.375 m, which is about 1/13 of the length L = 5 m of the beam, so that we are in the range of moderately large displacements.

Furthermore, we note that for decreasing amplitudes the frequency converges to the linear frequency ω_0= 290.56 rad/sec.

5. ANALYTICAL VERSUS NUMERICAL RESULTS

In this section, we compare the analytical (Sect. 3) with the numerical (Sect. 4) backbone curves, which is the major result of this paper.

We fix the slenderness of the beam, and vary the stiffness of the end spring. The results for L = 5 m and H = 50 cm (l = 34.610), and for L = 3 m and H = 50 cm (l = 20.7846) are reported in Figs. 3 and 4, respectively.

Since we are interested in comparing the nonlinear behaviour, i.e. the bending of the backbone curves, we found that it is convenient to shift a little bit the linear frequency of the analytical model to perfectly match the FEM one, so that the difference/agrement in the curvature of the backbones can be better appreciated from a graphical point of view. This is done by assuming $E = 2.110 \times 10^{11}$ N/m^2 in Fig. 3 and $E = 2.138 \times 10^{11}$ N/m^2 in Fig. 4 instead of the nominal value $E = 2.1{\times}10^{11}$ N/m^2. We remark that this is done only to better compare the curvatures of the analytical and numerical backbone curves, and not because we want to change the reference value of the Young modulus.

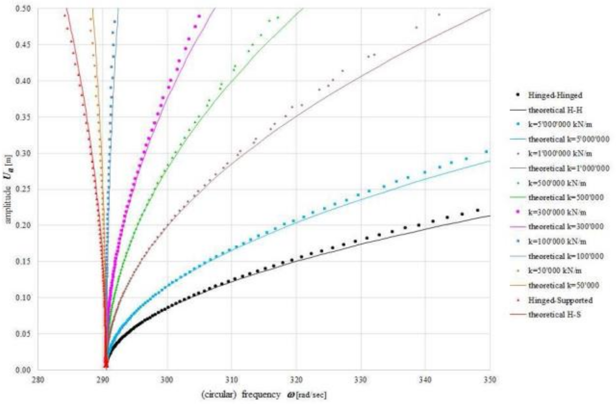

Figure 3 – Numerical (dots) vs analytical (lines) backbone curves for different values of the end spring stiffness κ. L = 5 m and H = 50 cm (l = 34.610).

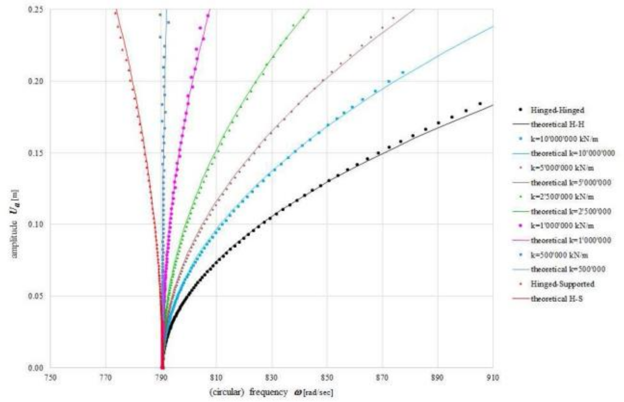

Figure 4 – Numerical (dots) vs analytical (lines) backbone curves for different values of the end spring stiffness κ. L = 3 m and H = 50 cm (l = 20.7846).

There is clearly a very good agreement between numerical and analytical approximations, in the whole range of end spring stiffnesses, from the hinged-supported (κ=0) to the hinged-hinged (κ→∞) cases. Also the transition from hardening to softening is well catched by both approximate solutions.

The minor differences visible for increasing amplitudes or for frequencies farther away from the linear one are likely due to the fact that the analytical solution is valid only up to the third order, while numerical simulations are valid everywhere.

6. CONCLUSIONS

The nonlinear free oscillations of a planar isotropic Timoshenko beam with axial end spring have been investigated by means of two different approximate solutions. Geometric nonlinearities are considered, while it is assumed that the material has a linear elastic behaviour.

The backbone curves, summarizing the nonlinear effects, have been determined in both cases, and compared to each other for two values of the beam slenderness. Very good agreement has been found in all cases.

The main developments of the study will consist of investigating numerically (a) the case of very low slenderness (l<10), and (b) higher order modes, and of comparing them with the analytical solution yet available.

References

[1] Atluri S., Nonlinear vibrations of hinged beam including nonlinear inertia effects. ASME J. Appl. Mech. 40, 121-126, 1973.
[2] Luongo A., Rega G., Vestroni F.: On nonlinear dynamics of planar shear indeformable beams. ASME J. Appl. Mech. 53, 619-624, 1986.
[3] Lacarbonara W., Yabuno H., Refined models of elastic beams undergoing large in-plane motions: Theory and experiments. Int. J. Solids Struct. 43, 5066-5084, 2006.
[4] Lenci S., Rega G., Nonlinear free vibrations of planar elastic beams: A unified treatment of geometrical and mechanical effects, IUTAM Procedia 19, 35-42, 2016.
[5] Lenci S., Clementi F., Rega G., A comprehensive analysis of hardening/softening behaviour of shearable planar beams with whatever axial boundary constraint. Meccanica, 2016, DOI: 10.1007/s11012-016-0374-6.
[6] Nayfeh A., 2004, Introduction to Perturbation Techniques, Wiley-VCH, ISBN: 0-978-471-31013-
[7] Kerschen G., Peeters M., Golinval J.C., Vakakis A.F., 2009, Nonlinear normal modes, Parts I & II, Mechanical Systems and Signal Processing, 23, 170–216.